Metal Ion Catalysis of RNA Cleavage by the Influenza Virus Endonuclease

Linh Doan, Balraj Handa, Noel A. Roberts, and Klaus Klumpp*

Roche Discovery Welwyn, 40 Broadwater Road, Welwyn Garden City, Herts AL7 3AY, U.K.

Received December 8, 1998; Revised Manuscript Received February 24, 1999

ABSTRACT: The influenza virus RNA-dependent RNA polymerase protein complex contains an associated RNA endonuclease activity, which cleaves host mRNA precursors in the cell nucleus at defined positions 9−15 nucleotides downstream of the cap structure. This reaction provides capped oligoribonucleotides, which function as primers for the initiation of viral mRNA synthesis. The endonuclease reaction is dependent on the presence of divalent metal ions. We have used a number of divalent and trivalent metal ions alone and in combination to probe the mechanism of RNA cleavage by the influenza virus endonuclease. Virus-specific cleavage was observed with various metal ions, and maximum cleavage activity was obtained with 100 μM Mn^{2+} or 100 μM Co^{2+}. This activity was about 2-fold higher than that observed with Mg^{2+} at the optimal concentration of 1 mM. Activity dependence on metal ion concentration was cooperative with Hill coefficients close to or larger than 2. Synergistic activation of cleavage activity was observed with combinations of different metal ions at varying concentrations. These results support a two-metal ion mechanism of RNA cleavage for the influenza virus cap-dependent endonuclease. The findings are also consistent with a structural model of the polymerase, in which the specific endonuclease active site is spatially separated from the nucleotidyl transferase active site of the polymerase module.

The influenza virus RNA-dependent RNA polymerase (RdRp)[1] is unique among all known polymerases to carry a cap-dependent endonuclease activity essential for transcription initiation. It is considered to be an attractive target for antiviral chemotherapy, and inhibitors of both polymerase and endonuclease activities have been described (*1*−*3*). For designing new compounds with improved potency and selectivity against this viral protein, a better characterization of the active sites of both polymerase and endonuclease functions will be crucial.

The influenza virus polymerase complex is a heterotrimer of three virus-encoded subunits PB1, PB2, and PA that carry the enzymatic activities required for transcription of the viral RNA in the nucleus of infected cells (*4*). The polymerase proteins are bound to the termini of nucleoprotein coated RNA gene segments of the virus, forming the viral ribonucleoprotein (RNP) (*5*−*7*). The binding of the polymerase to both ends of the viral genomic RNA is a prerequisite for the activation of endonuclease activity and transcription initiation (*8*, *9*). Viral mRNA synthesis starts with the binding of the activated polymerase complex to the cap structures of host pre-mRNAs, which are subsequently cleaved by the polymerase-associated endonuclease activity at distinct sites 9−15 nucleotides downstream of the cap (*10*−*13*). RNA cleavage by the influenza virus endonuclease generates 3′-hydroxyl and 5′-phosphate groups at the cleavage site. The resulting capped oligoribonucleotides are then used as primers for the initiation of transcription (*8*, *11*). Although the endonuclease activity of the influenza virus polymerase is essential for viral mRNA synthesis, the mechanisms of cleavage site choice and RNA cleavage itself as well as the location of the nuclease active site on the polymerase trimer are still unresolved. The active site may be located on the PB2 subunit, because PB2 contains the cap-binding site and specific anti-PB2 antibodies abolish the endonuclease activity in vitro. (*14*−*18*). However, endonuclease activity has only been observed with the complete complex of the three subunits PB1, PB2, and PA (*8*), and the cap-binding and endonuclease activities can be biochemically separated from each other on the basis of their distinct requirements of template RNA sequences (*19*). Therefore, at the moment conclusive evidence for the location of the endonuclease active site on any of the three subunits is still missing.

For a better understanding of how the influenza polymerase works and how it is related to cellular enzymes, it will be crucial to identify and characterize the active site that catalyzes RNA cleavage. As one step in this direction we have established an in vitro system to analyze the contribution of metal ions to the catalysis of phosphodiester bond hydrolysis by the influenza virus endonuclease. This work is interesting with respect to other metal-dependent nucleases. Until now, the present models of phosphodiester bond hydrolysis by metal-dependent nucleases have been based on only a small number of enzymes that contain either one or two divalent metal ions in the active site. The catalytic metal ions are coordinated by carboxyl side chains of highly conserved acidic amino acids. The identity and geometry of the coordinating amino acids are major factors that determine the metal-binding characteristics of nuclease active sites and are expected to affect the binding of potential inhibitor

* To whom correspondence should be addressed. E-mail: klaus.klumpp@roche.com.

[1] Abbreviations: RdRp, RNA-dependent RNA polymerase; RNP, ribonucleoprotein; NP, nucleoprotein; vRNA, viral, genomic RNA; TCA, trichloroacetic acid; nH, apparent Hill coefficient; Gem20-M, cap 1-(2′-methoxy)-Gem20 RNA; Gem20-H, cap 0-(2′-hydroxy)-Gem20 RNA.

10.1021/bi9828932 CCC: $18.00
Published on Web 04/06/1999

molecules to these enzymes. However, structural and functional studies of more nucleases are required to get a better understanding of the universality of this mechanism and its relation to active site architecture. Here, we studied single-stranded RNA cleavage by the influenza virus endonuclease under single-turnover conditions in the presence of different metal ions alone or in combination. The results are discussed with regard to the current models of metal ion-catalyzed RNA cleavage.

MATERIALS AND METHODS

Materials. Influenza virus A/PR/8/34 RNPs were prepared by standard procedures as described (*7*). RNP concentration was determined by spectroscopic determination of the RNA content after phenol extraction. Forty micrograms per milliliter was used as a conversion factor for 1 A_{260} unit of single-stranded RNA. Because polymerase activities were measured in a mixture of all eight viral genomic RNA segments, a mean RNA length of 1700 nucleotides (580 kD), packed with one nucleoprotein molecule per 20 nucleotides (4764 kD) and one polymerase complex (255 kD), was used to calculate RNP molarities in the activity assays (*4*). RNases for RNA sequencing and unlabeled ribonucleoside 5′-triphosphates were purchased from Pharmacia, *S*-adenosyl-L-methionine (SAM) and metal salts were from SIGMA, radiolabeled ribonucleotide 5′-triphosphates (3000 Ci/mmol) were from Amersham, and vaccinia virus guanylyltransferase was from Gibco BRL. Recombinant ribonuclease inhibitor RNasin was from Promega. Chloride salts of mono-, di-, and trivalent metal ions were purchased from SIGMA or Fluka in solid form, and aqueous solutions were freshly prepared prior to use. No corrections have been made for the partial loss of metal ions due to oxidation or the formation of insoluble metal hydroxides under the reaction conditions.

Synthesis of Capped RNAs. The endonuclease substrate used was Gem20 RNA, 5′-GAAUACUCAAGCUAUG-CAUC-3′. It contains the first twenty nucleotides of the previously described influenza virus endonuclease substrate GEM-RNA (*8*, *20*). The RNA oligonucleotides were chemically synthesized, phosphorylated, and enzymatically capped using vaccinia virus capping enzyme as described previously (*20*−*22*). Capped RNAs were purified by polyacrylamide gel electrophoresis using 15% gels containing 8 M urea. Gem20-M RNA contained a cap-1 structure with a 2′-methoxy group on the ribose of nucleotide 1, and Gem20-H RNA contained a cap-0 structure with a 2′-hydroxyl group on the ribose of nucleotide 1.

Endonuclease Assay. Except when indicated in the figure legends, endonuclease reactions were performed in 20 μL reaction mixtures containing 1.5 nM RNP, 50 mM Tris-HCl, pH 8, 100 mM KCl, 0.5 units/μL RNasin, 0.25 μg/μL BSA, 0.3% Triton × 100, and 15−150 pM ^{32}P-cap-labeled RNA. After incubation at 30 °C for 5−10 min, the reactions were ethanol precipitated by the addition of 180 μL of 0.3 M sodium acetate and 600 μL of ethanol. Precipitated samples were resuspended in 0.5 mM EDTA, 90% formamide, 0.1% (w/v) bromophenol blue, and 0.1% (w/v) xylene cyanol, denatured for 2 min at 98 °C, and loaded onto 20% acrylamide sequencing gels containing 7 M urea. Band intensities were quantified with a Storm PhosphorImager (Molecular Dynamics) using ImageQuant version 4.2a software. Initial reaction velocities were obtained and the data fitted to a plot of velocity, v, versus substrate concentration, [S], based on the Hill equation $v = [S]^{nH}V_{max}/[S]^{nH} + K_H$. Alternatively, plots of $\log(v/(V_{max} - v))$ versus log [S] were used to determine the apparent Hill coefficient, nH, from the equation $\log(v/(V_{max} - v)) = nH \log [S] - \log K_H$.

Cap-Dependent Transcription Assay. In the transcription assay 10−100 nM Gem20 RNA or rabbit globin mRNA (Life Technologies) was incubated with 1.5 nM RNP under the same buffer conditions as above, but including 5 mM $MgCl_2$, 50 μM CTP and GTP, 0.5 mM ATP, and 10 μM 3-H-UTP (0.04 μCi/μL). Reactions were incubated for 60 min at 30 °C, then precipitated with TCA, filter washed, and analyzed by scintillation counting as described previously (*20*).

For transcription initiation reactions, 1.5 nM RNP was incubated with 15−150 pM ^{32}P-cap-labeled Gem20 RNA and 10 μM CTP (1000K_m of CTP), in 50 mM Tris-HCl, pH 8, 100 mM KCl, 0.5 units/μL RNasin, 0.25 μg/μL BSA, and 0.3% Triton × 100 for 5−10 min at 30 °C. The products were analyzed on denaturing acrylamide gels as described above for endonuclease reactions.

RESULTS

Divalent Metal Ions Activate RNA Cleavage by the Influenza Virus Endonuclease in Vitro. To study the influenza virus endonuclease activity in vitro, we have used a new set of RNA oligonucleotides, Gem20-M and Gem20-H RNAs, derived from a previously characterized longer RNA, called GEM-RNA (*8*, *20*). We found that the capped RNA oligonucleotides were efficiently cleaved by the influenza virus endonuclease at the same nucleotide position 11 as was previously determined for GEM-RNA (Figure 1a). The endonuclease generates a capped 11-mer RNA called G11 that can be resolved on acrylamide gels (Figure 1b, lanes 7 and 12). G11 contains a 3′-OH and migrates more slowly in polyacrylamide gels compared with the corresponding RNase T1 cleavage product (G11-P), containing a 3′-phosphate group. In the presence of CTP, the G11 endonuclease product was efficiently used for transcription initiation by the influenza virus polymerase generating a G11+1nt product (Figure 1b, lanes 8 and 13). With Gem20 RNAs as substrates, both RNA cleavage and transcription inititiation were found to be dependent on the presence of Mg^{2+} ions (Figure 1 compare lanes 6 and 7, 8 and 9, 11 and 12, and 13 and 14). This was similar to previous reports by others using different RNA substrates (*22*, *23*). In agreement with results recently reported by Olsen et al., 1996, we also found that not phosphodiester bond cleavage but product release was rate-limiting under steady-state conditions also with our RNA substrates. To study the effect of metal ions on RNA hydrolysis, we therefore performed the current set of experiments in the presence of a 10−100-fold excess of enzyme in order to minimize the contribution of product dissociation on the cleavage rate. When the Gem20 RNA substrates were used, G11 product appeared to accumulate linearly with time up to 15 min, the initial cleavage rate being very similar using either Gem20-M or Gem20-H RNAs (Figure 1c). The cleavage rate showed a linear dependence on Gem20 RNA as expected under enzyme excess conditions (Figure 1d), whereas there was no change in cleavage rates

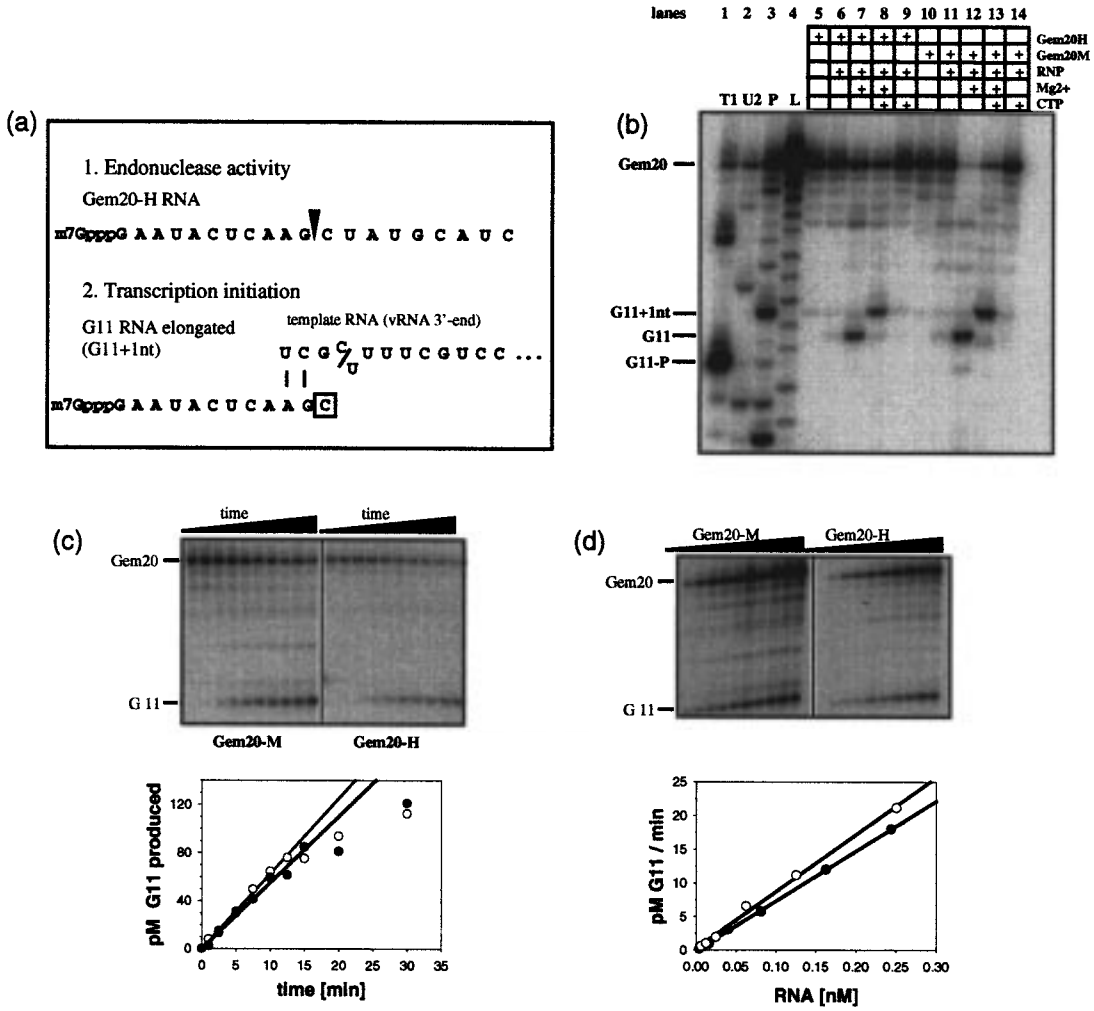

FIGURE 1: Capped Gem20 RNAs as endonuclease substrates. (a) Gem20 RNA sequence. The arrowhead indicates the specific cleavage site of influenza virus endonuclease to generate the capped G11 primer RNA. The G11 primer RNA can form two base pairs with the template RNA for transcription initiation. The polymerase initiates transcription with CMP incorporation as indicated by the boxed C. (b) The products of the endonuclease and transcription initiation reactions were analyzed on a denaturing polyacrylamide gel. Gem20 RNAs had been incubated in the presence or absence of either excess enzyme (RNP), 1 mM $MgCl_2$, or 10 μM CTP as indicated. Sequencing reactions of Gem20M RNA were performed with RNases T1, U2, and PhyM (P), selective for G, A, and A+U residues, respectively; L is an RNA ladder from alkaline hydrolysis of Gem20-M. The migration of the G11 RNA product of endonuclease, G11+1nt product of transcription initiation, and 3′-phosphorylated G11-P product of RNase T1 digestion relative to Gem 20 RNA is indicated on the left. (c) Time course of Gem20 RNA hydrolysis by the endonuclease, quantified by phosphorimager analysis from denaturing gels as described above. (d) Titration of Gem20-M and Gem20-H in the endonuclease reaction. Linear dependence of cleavage rate on RNA concentration shows that the RNA was rate-limiting under the assay conditions: white circles, Gem20-M; black circles, Gem20-H.

with RNP concentrations between 0.5 and 5 nM (not shown). From a range of metal ions, six divalent metal ions were found to activate specific RNA cleavage by the influenza virus endonuclease with $Mn^{2+} \approx Co^{2+} > Mg^{2+}$, Zn^{2+}, $Ni^{2+} > Fe^{2+}$ at their respective optimal concentrations (Table 1). Cd^{2+}, Ca^{2+}, Ba^{2+}, Sr^{2+}, and La^{3+} among others did not significantly activate cleavage at concentrations between 1 μM and 1 mM. Virtually identical results were obtained with either Gem20-M or Gem20-H RNAs. Because the methylation state of the first nucleotide of the capped RNA has been shown to influence cap-binding efficiency by the influenza virus polymerase complex (*24*), these results indicated that the cap-binding step was not rate-limiting in the current assay format. Also, none of the examined metal ions changed the cleavage site choice of the endonuclease. Specific cleavage occurred exclusively at position G11, and only the G11 primer was used for transcription initiation. A low background level of unspecific RNA degradation was observed under the reaction conditions employed, which was independent of RNA cap structures and the origin of which has not been investigated further.

RNA cleavage activity in the presence of Mg^{2+} was only observed at pH values above pH 6.5 and followed a saturation curve with OH^- concentration up to pH 9 consistent with an OH^- ion being the most likely nucleophile in the phosphodiester hydrolysis reaction (Figure 2). However, even at pH 9.2, the highest pH examined, the cleavage reaction was strictly dependent on the presence of the catalytic metal ion. If one role of the metal ions was to increase the local OH^- concentration in proximity of the active site, then metal ions with lower pK_a values would be expected to be able to activate RNA cleavage in lower pH environments. Accordingly, the titration curve was shifted to lower pH values in the presence of Mn^{2+}, an indication that the catalytic divalent metal ion could indeed be involved in the activation of the nucleophile (Figure 2). However, no further shift of the curve was observed for Co^{2+}, which has a lower pK_a than Mn^{2+} (Table 1). Also, the relative activation

Table 1: Screen of Metal Ions as Cofactors of the Influenza Virus Endonuclease and Transcription Activities

ionic radius [Å][a]	ion	nuclease activity[b]	transcription activity[c]	nH[d]	pK_a[e]
0.45	Be^{2+}	<1	nd	nd	5.7
0.54	Al^{3+}	<1	nd	nd	5
0.55	Fe^{3+}	<1	nd	nd	2.5
0.61	Fe^{2+}	10 ± 5	<1	nd	6.7
0.65	Co^{2+}	80 ± 6	<1	2 ± 0.2 (na)	8.9
0.67	Mn^{2+}	100	50 ± 15	4 ± 0.2 (2)	10.6
0.69	Ni^{2+}	40 ± 15	<1	1.5 ± 0.1 (na)	9.9
0.72	Mg^{2+}	49 ± 5	100	2 ± 0.1 (2)	11.4
0.73	Cu^{2+}	<1	nd	nd	7.3
0.74	Zn^{2+}	41 ± 15	<1	nd	9
0.95	Cd^{2+}	<1	nd	nd	9.3
1.00	Ca^{2+}	<1	nd	nd	12.6
1.02	Na^{+}	<1	<1	nd	15.7
1.16	La^{3+}	<1	nd	nd	9.1
1.26	Sr^{2+}	<1	nd	nd	13.1
1.42	Ba^{2+}	<1	nd	nd	13.4

[a] From ref *45*. [b] Relative endonuclease activities with standard deviations as determined from metal ion titrations and analysis of G11 production on acrylamide gels. The reactions were performed with 0.1 mM Mn^{2+}, Co^{2+}, Ni^{2+}, Fe^{2+}, Zn^{2+}, and 1 mM Mg^{2+}, that is, the apparent optimum concentrations for these metal ions for 10 min in the endonuclease assay at pH 8. None of the other metal ions showed significant activity above background at concentrations between 0.001 and 1 mM under these conditions. [c] Relative cap-dependent transcription activities determined as described in Materials and Methods. Optimum activity was obtained with 3.75 mM Mg^{2+} and 1 mM Mn^{2+} in the assay; nd, not determined. [d] Apparent Hill coefficient for metal ions in the endonuclease reaction as calculated from best-fit analysis of data from metal titration experiments. In brackets are the apparent Hill coefficients for the metal ions in the transcription assay; na, metal ion inactive in the transcription assay. [5] pK for hydrolysis of $Me^{n}+$, 25 °C (*46*).

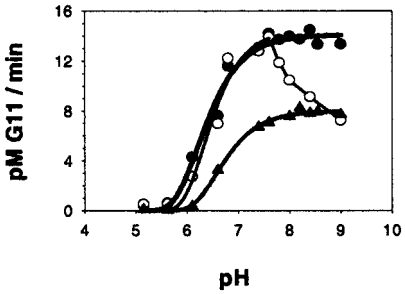

FIGURE 2: Dependence of RNA cleavage rate on pH. Endonuclease activity with Gem20-M RNA was measured at different pH values. Half-maximal activity was obtained at pH 6.8 in the presence of 1 mM $MgCl_2$ (black triangles, medium line), at pH 6.2 in the presence of 0.1 mM $MnCl_2$ (black circles, thick line), and at pH 6.2 in the presence of 0.1 mM $CoCl_2$ (white circles, thin line). The data were fitted to a double-exponential titration curve equation. Activity at optimal pH was about 2-fold higher with $MnCl_2$ and $CoCl_2$ as compared to $MgCl_2$ (see also Table 1).

of the endonuclease by the divalent metal ions at pH 8 did not appear to correlate with their respective pK_a values (Table 1). However, no corrections have been made for the influence of insoluble metal hydroxide formation on RNA cleavage, which could lead to an underestimation of cleavage rates with Ni^{2+} and Co^{2+}, nor to oxidation, which could influence the apparent cleavage rate in the presence of Fe^{2+} and Mn^{2+}. Cleavage activity was reduced with Co^{2+} at higher pH values due to increased precipitation under alkaline conditions (Figure 2). Half-maximal activation was observed at pH 6.8 with Mg^{2+} and pH 6.2 with Mn^{2+} and Co^{2+}.

The Binding of Divalent Metal Ions To Activate RNA Cleavage is Cooperative. The activation curves of the

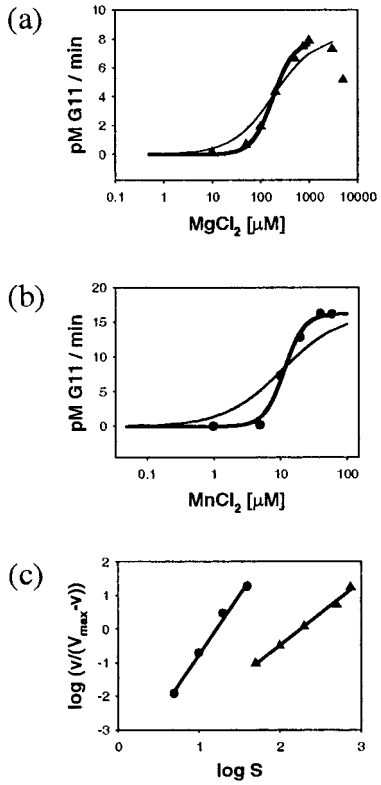

FIGURE 3: Cooperative effect of metal ion binding on endonuclease activity. Endonuclease assays were performed in the presence of increasing concentrations of $MgCl_2$ (a) or $MnCl_2$ (b). The reaction products were analyzed on polyacrylamide gels. The solid line shows the best fit of the data up to maximal activity to a Hill equation with an apparent Hill coefficient of 2 for $MgCl_2$ and 4 for $MnCl_2$. As a comparison, a least-squares fit of the same data to a noncooperative Hill equation with a fixed Hill coefficient of 1 is shown as a thin line. Note that the RNA cleavage activity was higher with $MnCl_2$ as compared to $MgCl_2$ in the assay. (c) Linear representation of the data according to the Hill equation plotting $\log(v/(V_{max} - v))$ versus $\log S$. S is the concentration of metal ions. Apparent Hill coefficients of 2 and 4 were obtained from linear regression analysis.

endonuclease reaction by the divalent metal ions were found to be sigmoid. To determine the degree of cooperativity, we fit the data to the Hill equation using the least-squares method (*25*). Figure 3 shows examples of Mg^{2+} and Mn^{2+} titrations, fitted curves, and the corresponding linear Hill plots. Hill coefficients of 2 and 4 were calculated for Mg^{2+} and Mn^{2+} from these data. In both cases the best-fit lines for presumed noncooperativity of metal ion binding have been included on the graphs for comparison (Figure 3, thin lines with fixed nH = 1). We also determined Hill coefficients for the activation of endonuclease activity with Co^{2+} (nH = 2) and Ni^{2+} (nH = 1.5). In all cases the apparent cooperativity of endonuclease activation upon metal ion binding suggested that at least two interacting metal-binding sites on the enzyme had to be filled with divalent metal ions to activate RNA cleavage. Activation by Mn^{2+} showed a significantly higher degree of cooperativity as compared to the other divalent metal ions, and Hill coefficients of 4 were reproducibly observed in several independent experiments (Figure 3).

We also determined the apparent Hill coefficients for the binding of the other substrates, capped RNA and NTP, to the polymerase complex. A cap-dependent transcription assay produced comparable results for either Gem20-M, Gem20-H, or globin mRNA as transcription primers. In contrast to

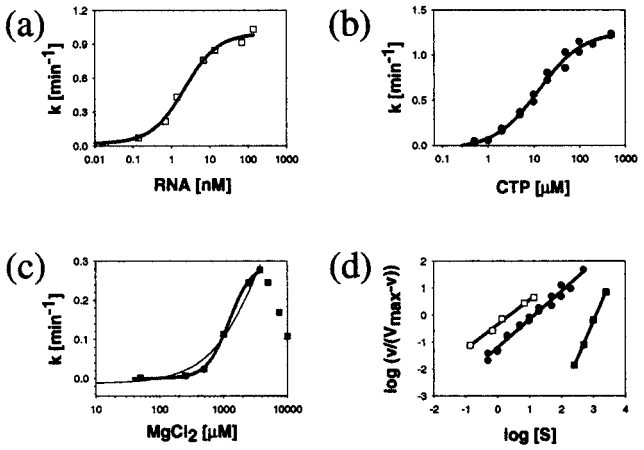

FIGURE 4: Substrate titrations in cap-dependent transcription reactions. (a) Dependence of influenza virus polymerase transcription activity on the concentration of Gem20-M RNA. Increasing amounts of RNA were titrated into a transcription assay using purified RNPs and tritiated UTP. The products of transcription were quantified after precipitation with TCA, filtration, and scintillation counting. Transcription rates *k* are expressed as nucleotide incorporations per enzyme molecule per minute. The data were fit to the Hill equation and resolved with an apparent Hill coefficient of 0.9. (b) Transcription activity in the presence of increasing amounts of CTP, analyzed as above, showed an apparent Hill coefficient of 1. (c) Transcription activity dependence on $MgCl_2$. The data up to maximal activity were fit to the Hill equation, and a Hill coefficient of 2 was deduced from the best fit (thick line). As a comparison, a best-fit line with a fixed nH of 1 is shown on the graph (thin line). (d) The data of a, b, and c were plotted according to the linear Hill equation as described in Figure 3. Linear regression analysis is shown and gave nH values of 0.9, 1, and 2 for Gem 20-M RNA (white squares), CTP (black circles), and $MgCl_2$ (black squares), respectively.

the endonuclease reaction, the complete transcription activity was only observed in the presence of either Mg^{2+} or Mn^{2+}, but not with either Co^{2+}, Zn^{2+}, Ni^{2+}, or Fe^{2+} (Table 1). Also, metal ion preference was changed with 3.75 mM Mg^{2+}, conferring significantly higher transcription activity than Mn^{2+} at the optimal concentration of 1 mM. The Hill coefficients obtained were nH = 2 for both Mg^{2+} and Mn^{2+} (Table 1 and Figure 4a). In contrast to the results obtained with the metal ion titration experiments, nH was 1 for capped RNA substrate under steady-state conditions of capped RNA primed transcription (Figure 4b). Hill coefficients of 1 were also calculated for each of the four NTPs in the transcription assay (Figure 4c). These observations are consistent with a model of the polymerase complex containing one binding site for capped RNA substrate and one binding site for the nucleotide triphosphates on the polymerase complex. However, metal ion requirements were different for RNA cleavage and transcription activities, and at least two metal ion-binding sites appear to be involved in each process. Of the best characterized nucleases, most are supposedly using either a one-metal or a two-metal ion mechanism of phosphodiester bond hydrolysis (*26*, *27*). To determine if the metal ion-binding sites on the influenza virus endonuclease are functionally coupled as predicted by the two-metal ion mechanism of nucleic acid cleavage (*28*), we made use of the fact that we had observed cleavage activation by several different divalent metal ions.

Low Concentrations of Mn^{2+} Synergistically Enhance RNA Cleavage in the Presence of Mg^{2+}. In the two-metal ion mechanism of phosphodiester bond cleavage as has been

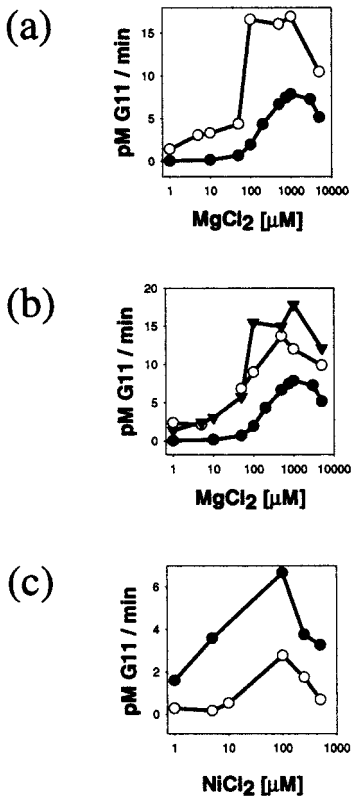

FIGURE 5: Synergistic activation of RNA cleavage in the presence of combinations of different metal ions. Endonuclease reactions were performed and analyzed on acrylamide gels as described above. (a) Endonuclease reactions in the presence of $MnCl_2$ fixed at 1 μM and increasing concentrations of $MgCl_2$ (white circles) compared to reactions with increasing amounts of $MgCl_2$ only (black circles). (b) Endonuclease reactions in the presence of increasing concentrations of $MgCl_2$ and fixed $NiCl_2$ at 10 μM (white circles) or fixed $CoCl_2$ at 1 μM (black triangles) as compared to reactions with increasing amounts of $MgCl_2$ only (black circles). (c) Endonuclease reactions in the presence of increasing concentrations of $NiCl_2$ and fixed $MgCl_2$ at 100 μM (black circles) as compared to reactions with increasing amounts of $NiCl_2$ only (white circles). In all cases higher cleavage rates could be obtained under mixed metal conditions than would be expected from the activities of both metal ions alone.

proposed for ribozymes and the DNase activity of Klenow fragment (*28*), one metal ion is involved in activating the attacking nucleophile and orienting the reactive trigonal face of the tetrahedral phosphate by interacting with a nonbridging oxygen of the phosphate. The second metal ion is interacting with the leaving group and electrostatically stabilizes the negative charge on the 3′ hydroxyl of the cleaved product. As discussed by Lott et al. (*29*), considering the different functions of the two metal ions in the hydrolysis reaction, it is unlikely that a single metal ion could function optimally at both binding sites. We therefore studied RNA cleavage by the influenza virus endonuclease in the presence of increasing Mg^{2+} concentrations at constant Mn^{2+} concentrations. With Mn^{2+} at 1 or 10 μM, additional Mg^{2+} enhanced the cleavage reaction synergistically above the rates observed with either Mn^{2+} or Mg^{2+} alone (Figure 5a). This suggested that, at suboptimal concentrations of Mn^{2+}, simultaneous binding of both Mn^{2+} and Mg^{2+} resulted in significantly increased activity of the enzyme as compared to filling the metal ion-binding sites with Mg^{2+} alone. A similar enhancement of cleavage rates was observed with Ni^{2+} and Co^{2+} in combination with Mg^{2+} (Figure 5b,c). We also screened the

metal ions that had not activated the endonuclease in isolated form for an activating or inhibiting effect when added to reactions containing either optimal (1 mM) or suboptimal (0.1 mM) concentrations of Mg^{2+}. However, none of the endonuclease nonactivating metal ions showed any positive or negative effect on Mg^{2+}-catalyzed RNA cleavage when assayed at concentrations between 1 μM and 1 mM. This suggested that either the endonuclease nonactivating metal ions were unable to bind to the enzyme or they bound to a site that did not interfere with endonuclease activity conferred by the filling up of the interacting Mg^{2+}-binding sites.

DISCUSSION

In this study we have started to characterize the role of divalent metal ions for the process of RNA cleavage by the endonuclease activity of the influenza virus RNA-dependent RNA polymerase. Six divalent metal ions showed significant activation of RNA cleavage. They cover an ionic size window of 0.61−0.74 Å. Interestingly, larger metal ions such as Cd^{2+}, Ca^{2+}, Sr^{2+}, or Ba^{2+} that have been shown to be able to replace Mg^{2+} in the active sites of other nucleases were inactive in this system. Because in addition they showed neither activating nor inhibiting effects on Mg^{2+}-catalyzed RNA cleavage, they may be too large to fit into the influenza virus endonuclease metal-binding sites. To our knowledge, an identical metal ion preference has not been reported for any other nuclease so far. In addition, the activation characteristics of the influenza virus endonuclease by metal ions are different from the metal ion requirements of the nucleotide transferase site during transcription elongation. Of all the metal ions tested only two, Mg^{2+} and Mn^{2+}, also significantly activated RNA-dependent transcription activity with the influenza virus polymerase. However, metal ion preference was different in this case, as the yield of full-length transcripts was significantly higher with Mg^{2+} as compared to Mn^{2+} (*30*). These observations are consistent with the existence of distinct active sites for RNA cleavage and RNA synthesis that are physically separated on the protein complex. This is in agreement with previous studies showing the existence of specific endonuclease inhibitors that specifically prevent RNA cleavage activity, but not dinucleotide primed (endonuclease-independent) transcription activity of the influenza virus polymerase complex (*3, 31*).

In the cases where cleavage rate analysis over large ranges of metal ion concentrations was possible, the metal ions were found to activate the endonuclease in a cooperative fashion with Hill coefficients larger than 1. This indicates that at least two interacting metal-binding sites for these metal ions are present on the protein. Although the easiest explanation for these results is that two interacting binding sites are present within the endonuclease active site, long-range allosteric effects from metal ion-binding sites spatially separated from the endonuclease site could not be excluded. In particular, because the influenza virus polymerase complex appears to contain two separate active sites for RNA cleavage and RNA synthesis, both could bind metal ions and the insertion of one metal ion into each site could be required for endonuclease activation. For nucleic acid synthesis sites on polymerases, based on the known crystal structures of DNA polymerases and one DNA-dependent RNA polymerase, a common mechanism of nucleic acid synthesis involving two divalent metal ions in the catalytic site has been proposed that may be similar for all polymerases (*32, 33*). Consistent with this view, the important metal chelating amino acids are highly conserved among all polymerases. The corresponding amino acids of the influenza virus polymerase complex have been identified on the primary sequence of PB1 and shown by mutagenesis to be essential for transcription activity (*34*).

However, more evidence for two additional metal ions binding to a separate endonuclease site on the influenza virus polymerase complex was obtained from experiments with Mn^{2+} as the activating metal ion. The binding of Mn^{2+} to the protein was different from the other metal ions with Mn^{2+} activation of RNA cleavage showing cooperativity with a Hill coefficient of 4, suggesting at least 4 interacting Mn^{2+}-binding sites on the protein. Presuming that the endonuclease and the nucleotidyl transferase sites are confined to two distinct domains, the present results are most easily explained by a model where Mn^{2+} fills up both the nucleotidyl transferase site and the endonuclease site with two metal ions each in a coordinated fashion. Consistent with this model, Mn^{2+} did activate both RNA cleavage and RNA synthesis activity of the protein complex; that is, Mn^{2+} ions could productively bind into both active sites. The observation of a cooperativity of 4 for the bifunctional Mn^{2+} and 2 for Co^{2+}, Fe^{2+}, and Ni^{2+}, which did not support transcription activity and may therefore be unable to bind into the nucleotidyl transferase site, suggested that at least two interacting binding sites independent of the nucleotidyl transferase site were involved in RNA cleavage activity. Apart from Mn^{2+}, Mg^{2+} is the only metal ion that also supports both nucleotidyl transferase and endonuclease activities of the influenza virus polymerase complex. Mg^{2+} is therefore also expected to fill all 4 metal ion-binding sites, when present as the only divalent metal ion in the reaction, but in this case only 2 binding sites show a cooperative effect during RNA cleavage activation.

Further evidence for a direct interaction of two metal ion-binding sites in the chemical step of RNA cleavage came from mixing experiments of two different metal ions. As predicted by the two-metal ion model for nucleic acid hydrolysis, two different metal ions could synergistically enhance RNA cleavage because of the differing functions for each metal ion in the catalytic process. In the case of the influenza virus endonuclease, we observed synergistic activation of cleavage when Mg^{2+} was combined with either Mn^{2+}, Co^{2+}, Ni^{2+}, or Fe^{2+}. At present it is unclear if a similar activation of RNA cleavage could also be achieved by metal−nucleic acid interactions, if a second metal ion species was promoting a more competent cleavage form of the substrate. However, the observed metal ion selectivity and the high cooperativity of the cleavage reaction do argue against this possibility.

Nucleic acid cleavage enhancements by mixtures of metal ions have previously been reported for the activation of ribozymes and indicated the concerted action of two metal ions during the ribozyme cleavage reaction. The HH16 hammerhead ribozyme was optimally activated by a combination of 3 μM La^{3+} and 8 mM Mg^{2+} (*29*), the leadzyme ribozyme by a combination of Pb^{2+} and Nd^{3+} (*35*). Synergistic activation of nucleic acid cleavage by proteins in the presence of metal ion combinations has been reported at least once before. *Eco*RV and *Eco*RI, two of the best characterized

metal-dependent restriction enzymes, both showed noncooperative binding of Mg^{2+} (*36*). They had maximal activity in the presence of Mg^{2+} but were also significantly active with Mn^{2+} (about 10-fold less active). *Eco*RV but not *Eco*RI showed synergistic activation in the presence of Mn^{2+} and Ca^{2+}, whereas Ca^{2+} strongly inhibited Mg^{2+}-activated DNA cleavage with both enzymes (*37*). Consistent with these findings, the corresponding crystal structures soaked in the presence of metal ions showed one Mn^{2+} ion bound to each monomer of *Eco*RI, but two Mg^{2+} ions bound to *Eco*RV in the crystals (*38*, *39*). On the basis of these results, a two-metal ion model was proposed as the most likely mechanism for DNA cleavage by *Eco*RV and a one-metal ion mechanism for cleavage by *Eco*RI. Enzyme inhibition and binding of two Ca^{2+} ions into the active site has also been found for *Bam*HI (*40*). As mentioned above, Ca^{2+} up to 1 mM concentration did not have any effect, stimulating or inhibiting, on the influenza virus endonuclease activity, and both Co^{2+} and Mn^{2+} stimulated RNA cleavage activity more than Mg^{2+}, indicating significant differences in active site architecture between the DNA endonucleases and the influenza virus RNA endonuclease.

In other studies of enzyme-catalyzed DNA hydrolysis reactions, Mn^{2+} has sometimes been found to induce an increase of nonspecific cleavages. For example a number of restriction endonucleases show star activity in the presence of Mn^{2+}, that is, reduced cleavage site discrimination leading to additional cleavage at noncognate sites. This is in contrast to the influenza virus endonuclease, which cleaved the capped Gem20 RNA substrate specifically at position G11 with any of the six activity conferring metal ions. We have not seen any evidence for changes in cleavage site choice related to the ionic conditions of the influenza virus endonuclease reaction buffers with these substrates.

Taken together, the cooperative effect of metal ion binding on RNA cleavage activity of the influenza virus endonuclease and the synergistic activation of cleavage in the presence of two different species of metal ions suggest a two-metal ion mechanism of phosphodiester bond hydrolysis for this reaction. The different metal ion requirements also support the model of two independent two-metal ion active sites on the Influenza virus polymerase complex. Similar enzymes with two active sites both containing metal ion-binding sites have been described before. Many DNA polymerases contain associated nuclease domains that most likely use a two-metal ion module for DNA cleavage (*41*). These exonuclease domains are involved in the proofreading process of DNA polymerases. However, in contrast to these nuclease domains, the influenza virus endonuclease appears to be restricted to RNA cleavage at distinct sites on the substrate RNAs by the dependence on a cap structure in a defined distance from the cleavage site. From this it seems unlikely that the endonuclease would be involved in proofreading processes during transcription elongation. However, evidence for a possible proofreading activity of the influenza virus polymerase complex at early stages of transcription has been reported before (*42*). After the discovery of proofreading exonuclease functions of RNA polymerase II and *Escherichia coli* RNA polymerase (*43*, *44*), this potential aspect of influenza virus endonuclease activity still requires further investigation. The present in vitro system of endonuclease activity will be useful to study the potential involvement of the endonuclease active site at early and later stages of RNA synthesis by the influenza virus RNA polymerase.

REFERENCES

1. Meanwell, N. A., and Krystal, M. (1996) *Drug Discovery Today 1*, 388−397.
2. Tisdale, M., Ellis, M., Klumpp, K., Court, S., and Ford, M. (1995) *Antimicrob. Agents Chemother. 39*, 2454−2458.
3. Tomassini, J., Selnick, H., Davies, M. E., Armstrong, M. E., Baldwin, J., Bourgeois, M., Hastings, J., Hazuda, D., Lewis, J., McClements, W., Ponticello, G., Radzilowski, E., Smith, G., Tebben, A., and Wolfe, A. (1994) *Antimicrob. Agents Chemother. 38*, 2827−2837.
4. Lamb, R. A., and Krug, R. M. (1996) in *Fields Virology* (Fields, D. M., et al., Eds.) pp 1353−1445, Lippincott-Raven Publishers, Philadelphia, PA.
5. Hsu, M. T., Parvin, J. D., Gupta, S., Krystal, M., and Palese, P. (1987) *Proc. Natl. Acad. Sci. U.S.A. 84*, 8140−8144.
6. Honda, A., Mukaigawa, J., Yokoiyama, A., Kato, A., Ueda, S., Nagata, K., Krystal, M., Nayak, D. P., and Ishihama, A. (1990) *J. Biochem. 107*, 624−628.
7. Klumpp, K., Ruigrok, R. W. H., and Baudin, F. (1997) *EMBO J. 16*, 1248−1257.
8. Hagen, M., Chung, T. D., Butcher, J. A., and Krystal, M. (1994) *J. Virol. 68*, 1509−1515.
9. Fodor, E., Pritlove, D. C., and Brownlee, G. G. (1994) *J. Virol. 68*, 4092−4096.
10. Plotch, S. J., Bouloy, M., and Krug, R. M. (1979) *Proc. Natl. Acad. Sci. U.S.A. 76*, 1618−1622.
11. Plotch, S. J., Bouloy, M., Ulmanen, I., and Krug, R. M. (1981) *Cell 23*, 847−858.
12. Caton, A. J., and Robertson, J. S. (1980) *Nucleic Acids Res. 8*, 2591−2603.
13. Beaton, A. R., and Krug, R. M. (1981) *Nucleic Acids Res. 9*, 4423−4436.
14. Blaas, D., Patzelt, E., and Kuechler, E. (1982) *Nucleic Acids Res. 10*, 4803−4812.
15. Blok, V., Cianci, C., Tibbles, K. W., Inglis, S. C., Krystal, M., and Digard, P. (1996) *J. Gen. Virol. 77*, 1025−1033.
16. Shi, L., Summers, D. F., Peng, Q., and Galarza, J. M. (1995) *Virology 208*, 38−47.
17. Ulmanen, I., Broni, B. A., and Krug, R. M. (1981) *Proc. Natl. Acad. Sci. U.S.A. 78*, 7355−7359.
18. Ulmanen, I., Broni, B. A., and Krug, R. M. (1983) *J. Virol. 45*, 27−35.
19. Cianci, C., Tiley, L., and Krystal, M. (1995) *J. Virol. 69*, 3995−3999.
20. Klumpp, K., Ford, M. J., and Ruigrok, R. W. (1998) *J. Gen. Virol. 79*, 1033−1045.
21. Brownlee, G. G., Fodor, E., Pritlove, D. C., Gould, K. G., and Dalluge, J. J. (1995) *Nucleic Acids Res. 23*, 2641−2647.
22. Olsen, D. B., Benseler, F., Cole, J. L., Stahlhut, M. W., Dempski, R. E., Darke, P. L., and Kuo, L. C. (1996) *J. Biol. Chem. 271*, 7435−7439.
23. Chung, T. D., Cianci, C., Hagen, M., Terry, B., Matthews, J. T., Krystal, M., and Colonno, R. J. (1994) *Proc. Natl. Acad. Sci. U.S.A. 91*, 2372−2376.
24. Bouloy, M., Plotch, S. J., and Krug, R. M. (1980) *Proc. Natl. Acad. Sci. U.S.A. 77*, 3952−3956.
25. Dixon, M., and Webb, E. C. (1979) in *Enzymes*, Longman Group Ltd., London, U.K.
26. Wilcox, D. E. (1996) *Chem. Rev. 96*, 2435−2458.
27. Cowan, J. A. (1998) *Chem. Rev. 98*, 1067−1087.
28. Steitz, T. A., and Steitz, J. A. (1993) *Proc. Natl. Acad. Sci. U.S.A. 90*, 6498−6502.
29. Lott, W. B., Pontius, B. W., and von Hippel, P. H. (1998) *Proc. Natl. Acad. Sci. U.S.A. 95*, 542−547.
30. Plotch, S. J., and Krug, R. M. (1977) *J. Virol. 21*, 24−34; Klumpp, K., et al. (manuscript in preparation).
31. Cianci, C., Chung, T. D. Y., Meanwell, N., Putz, H., Hagen, M., Colonno, R. J., and Krystal, M. (1996) *Antiviral Chem. Chemother. 7*, 353−360.

32. Doublie, S., Tabor, S., Long, A. M., Richardson, C. C., and Ellenberger, T. (1998) *Nature 391*, 251−258.
33. Steitz, T. A. (1998) *Nature 391*, 231−232.
34. Biswas, S. K., and Nayak, D. P. (1994) *J. Virol. 68*, 1819−1826.
35. Ohmichi, T., and Sugimoto, N. (1997) *Biochemistry 36*, 3514−3521.
36. Jeltsch, A., Alves, J., Wolfes, H., Maass, G., and Pingoud, A. (1993) *Proc. Natl. Acad. Sci. U.S.A. 90*, 8499−8503.
37. Vipond, I. B., Baldwin, G. S., and Halford, S. E. (1995) *Biochemistry 34*, 697−704.
38. Rosenberg, J. M. (1991) *Curr. Opin. Struct. Biol. 1*, 104−113.
39. Kostrewa, D., and Winkler, F. K. (1995) *Biochemistry 34*, 683−696.
40. Viadiu, H., and Aggarwal, A. K. (1998) *Nat. Struct. Biol. 5*, 910−916.
41. Beese, L. S., and Steitz, T. A. (1991) *EMBO J. 10*, 25−33.
42. Ishihama, A., Mizumoto, K., Kawakami, K., Kato, A., and Honda, A. (1986) *J. Biol. Chem. 261*, 10417−10421.
43. Reines, D. (1994) in *Transcription: Mechanisms and Regulation* (Conaway R. C., and Conaway, J. W., Eds.) pp 263−278 Raven Press, New York.
44. Thomas, M. J., Platas, A. A., and Hawley, D. K. (1998) *Cell 93*, 627−637.
45. Evans, H. T. (1995) in *CRC Handbook of Chemistry and Physics* (Lide, D. R., Ed.) pp 12.14−12.15, CRC Press, Boca Raton, FL.
46. Perrin, D. D. (1982) in *Ionisation constants of inorganic acids and bases in aqueous solution*, Pergamon Press Ltd., Oxford, U.K.

BI9828932